Analyst

Carbon-carbon double bond position elucidation in fatty acids using ozone-coupled direct analysis in real time mass spectrometry

Journal:	*Analyst*
Manuscript ID	AN-ART-06-2019-001059.R1
Article Type:	Paper
Date Submitted by the Author:	21-Aug-2019
Complete List of Authors:	Cetraro, Nicolas; University of Hawai'i at Manoa, Pacific Biosciences Research Center Cody, Robert; Jeol USA Inc Yew, Joanne; University of Hawai'i at Manoa, Pacific Biosciences Research Center

Carbon-carbon double bond position elucidation in fatty acids using ozone-coupled direct analysis in real time mass spectrometry

Short title: **Ozone-coupled DART MS**

Nicolas Cetraro[1], Robert B. Cody[2], Joanne Y. Yew[1*]

[1] Pacific Biosciences Research Center, University of Hawai‘i at Mānoa; 1993 East West Road, Honolulu, USA 96822

[2]JEOL USA, Inc.; 11 Dearborn Rd, Peabody, MA, USA 01960

*corresponding author:
Joanne Y. Yew
1993 East West Rd
Honolulu, HI 96822
808-956-5870
jyew@hawaii.edu

Abstract

The carbon-carbon double bond positions of unsaturated fatty acids can have markedly different effects on biological function and also serve as biomarkers of disease pathology, dietary history, and species identity. As such, there is great interest in developing methods for the facile determination of double bond position for natural product chemistry, the pharmaceutical industry, and forensics. We paired ozonolysis with direct analysis in real time mass spectrometry (DART MS) to cleave and rapidly identify carbon-carbon double bond position in fatty acids, fatty alcohols, wax esters, and crude fatty acid extracts. In addition, ozone exposure time and DART ion source temperature were investigated to identify optimal conditions. Our results reveal that brief, offline exposure to ozone-generated aldehyde and carboxylate products that are indicative of carbon-carbon double bond position. The relative abundance of diagnostic fragments quantitatively reflects the ratios of isobaric fatty acid positional isomers in a mixture with a correlation coefficient of 0.99. Lastly, the unsaturation profile generated from unfractionated, fatty acid extracts can be used to differentiate insect species and populations. The ability to rapidly elucidate lipid double bond position by combining ozonolysis with DART MS will be useful for lipid structural elucidation, assessing isobaric purity, and potentially distinguishing between animals fed on different diets or belonging to different ecological populations.

Introduction

Lipids play a broad range of physiological and behavioral functions in cellular signaling[1], membrane architecture[2, 3], and chemical communication[4]. Moreover, changes in lipid composition are used as markers for human disease[5-10]. In each of these biological processes, the molecular composition, stereochemistry, and the degree and sites of unsaturation can contribute significantly to the functional properties of lipids. Elucidating the absolute structure of lipid molecules is thus critical for our understanding of basic biological functions, ligand-receptor interactions, and drug design.

Carbon-carbon double bond position is an important structural feature of lipids that can provide significant insight into underlying biochemical synthesis pathways[11-13], and serve as an indicator of food purity[14], disease pathology[15, 16], and dietary intake[17, 18]. Numerous methods have been devised for the facile elucidation of double bond position in lipids. Early approaches used charge remote fragmentation to analyze underivatized fatty acids (FAs). High energy collision-induced dissociation (CID)[19, 20] or low energy CID of FAs with dilithium adducts produced a series of fragments indicative of carbon-carbon double bond positions[21, 22]. When applied to triacylglycerides, the identity of each acyl group, position on the backbone, and location of double bond within each acyl group could be determined. With a sufficiently narrow *m/z* isolation window, it is possible to use high energy CID to obtain full structural elucidation from individual TAG species within a complex mixture[23]. More recently, radical-induced dissociation using hydrogen abstraction and oxygen attachment dissociation was shown to be an effective method for the assignment of double bond positions within fatty acyl chains of phospholipids[24]. With each of these ion activation methods, no derivatization is needed, thus minimizing quantitative variation and spectral complexity due to incomplete or side reactions. However, complete structural elucidation requires a relatively high amount of starting material (approximately 10 - 100 μM).

A second strategy for carbon-carbon double bond elucidation implements online chemical cleavage or conversion to a functional group followed by CID to produce fragments that are diagnostic for sites of unsaturation. Plasma-based probes have been used to epoxidize fatty acid samples offline[25] or placed on paper strips[26]. Another plasma-based method, atmospheric

pressure covalent adduct chemical ionization (APCACI), covalently modifies TAGs with acetonitrile-derived ions at the carbon-carbon double bond[27]. Modification of carbon-carbon double bonds has also be achieved using an online UV photochemical reaction, Paternò Büchi (PB), which adds an acetone radical to carbon-carbon double bonds, forming an oxetane[28]. With each of these methods, subsequent fragmentation by CID of the converted molecule generates fragments indicative of double bond position. With each of these methods, The PB method has been paired with shot gun lipidomics[29], liquid chromatography (LC) MS[30, 31], and matrix-assisted laser desorption/ ionization MS imaging[32] towards the characterization of glycerophospholipids, cholesterol esters, and FAs in complex mixtures and tissue sections. Notably, Ma et al. (2016) showed that the relative ratios of diagnostic ion abundance can be used to quantify the abundance of lipid regioisomers. Each of these online conversion methods is fast, compatible with high throughput analysis, and can be coupled with MS instruments without extensive modification. While epoxidation provides up to 95% reaction yields for monounsaturated FAs, APCACI and PB generate up to 70% or 40-60% yields, respectively. The incomplete conversion results in lower yields of target molecules and can complicate spectra and absolute quantitation.

Ozone-based chemistry has also been successfully coupled with mass spectrometry for structural elucidation. Ozone reacts rapidly with carbon-carbon double bonds to generate an ozonide intermediate which, upon oxidation or reduction, leads to the formation of carboxylic acids and aldehydes with carbon chain lengths diagnostic of the original double bond position[33]. Several offline methods of derivatization have been reported. Harrison and Murphy used electrospray ionization mass spectrometry coupled with CID to determine the FA double bond positions of glycerolipids[34]. Following offline exposure to ozone vapor, ozonides were isolated and decomposed by CID, thus allowing diagnostic fragments to be assigned to individual lipid species. Ozone produced inside a chamber[35] or generated with a low temperature plasma probe[36] can also be used to analyze products from thin layer chromatography plates and other surfaces. Offline methods work best with few component mixtures, allowing for rapid profiling with minimal sample preparation and loss, and requires no modification of the instrument. However, without chromatographic separation of parent ions or precursor selection prior to cleavage, the analysis of complex mixtures is challenging since ozone-produced cleavage products complicate

the spectra and diagnostic ions cannot reliably be assigned to the parent ions from which they were derived.

By contrast, the online coupling of ozonolysis with LCMS and/ or MS/MS analysis allows for complex mixture analysis. A number of ozonolysis induction methods have been demonstrated to be compatible with online analysis in recent years. Ozone-induced dissociation (OzID), exposes mass-selected ions to ozone in the gas phase within the ion trap or collision cell of various MS platforms[37-41], requires no external derivatization or CID step, and can be paired with LC[42] for on-line identification of double bond isomers. The branching ratio of the product ions generated by OzID can also be used to differentiate *cis* vs. *trans* geometry with careful calibration[43]. Ozonolysis of oleic acid, phosphotidylglycerols, and sterols from the surface of microliter droplets followed by field-induced droplet ionization MS is an effective method for examining oxidative reactions at the air-liquid interface[44, 45]. Photochemical derivatization using a UV lamp placed near a nanoESI emitter serves an ozone source capable of cleaving lipid standards[46]. Several solution-phase reaction chamber designs have been devised that provide ozone exposure to samples following chromatographic separation and results in the production of diagnostic aldehyde ions from FA, phospholipids, and crude extract mixtures prior to MS analysis[47-50]. The use of a reaction chamber allows flow speed and ozone exposure to be controlled. At lower flow rates, up to 95% conversion is observed. Finally, ozonolysis has been induced through the use of radical probe MS. Hydroxyl radicals are generated by applying an electrical discharge within an electrospray ion source. The oxidation profile of amino acid side chains has been used to elucidate protein structural features and examine protein interactions.[51]

Here we couple offline ozonolysis with an ambient ionization method, Direct Analysis in Real Time (DART) MS, to analyze lipid mixtures and natural lipid extracts derived from insects. We show that in the absence of subsequent reductive and oxidative workup steps or collision induced dissociation, this method is effective for i) revealing carbon-carbon double bond position in fatty acids, fatty alcohols, and wax esters, ii) determining the relative abundance of isomeric unsaturated fatty acid species in a mock mixture, and iii) distinguishing between closely related populations of animals based on the fatty acid unsaturation profile as a form of chemical fingerprinting.

Experimental

Materials

Linoleic acid, oleic acid, trioleyl glycerol, and methylene chloride were obtained from Sigma-Aldrich (St. Louis, MO, USA). Conjugated linoleic acid and vaccenic acid were purchased from Cayman Chemicals (Ann Arbor, Michigan, USA). The fruit fly pheromone CH503 ((3*R*,11*Z*,19*Z*)-3-acetoxy-11,19-octacosadien-1-ol) was previously synthesized [52]. All standards were dissolved in hexane at 1 mM concentration, unless otherwise stated.

Animals

Five Hawaiian *Drosophila* species were used: *D. silvestris* (two populations: from the eastern side of Hawaii Island, Saddle Road (N19 40.202, W155 20.142); and from the western side, South Kona Forest Reserve (N19 18.447, W155 49.098). *D. hawaiiensis, D. grimshawi, D. differens,* and *D. heteroneura* Collections were made at the Koke‘e State Park and Kui‘a Natural area reserve on Kauai, West Maui Forest Reserve, Makawao Forest Reserve, the Nature Conservancy’s Waikamoi Preserve on Maui, and Hawai‘i Volcanoes National Park and Upper Waiakea Forest Reserve on Hawai‘i Island. *Drosophila* were raised on Clayton-Wheeler diet [53] at 19 °C. Each species has been maintained under laboratory conditions for at least 24 generations.

Fatty acid extracts

Fatty acids were extracted from homogenates of whole female *Drosophila* in chloroform/ methanol (1:2, v/v) for 3 hours at 4 °C with constant agitation. Three to five replicates consisting of 2-3 flies each were prepared for each species or population member. The supernatant was removed and the crude homogenate re-extracted two more times using chloroform. The pooled supernatant was evaporated to dryness under a gentle stream of N_2. Methyl esterification was performed by exposure to methanolic HCl (Sigma-Aldrich, #33355) for 1 hour at 65 °C, followed by evaporation of the solvent. Prior to analysis, the esterified samples were dissolved in 100 μL of hexane spiked with 10 μg/ mL pentadecanoic acid. Methyl esterification is not

necessary for DART MS analysis but was performed for gas chromatography MS (GCMS) experiments.

Mass spectrometry

DART MS Mass spectra were acquired with an atmospheric pressure ionization time-of-flight mass spectrometer (AccuTOF-DART 4G, JEOL USA, Inc., Peabody, MA) equipped with a DART SVP ion source interface (IonSense LLC, Saugus, MA), placed 1 cm away from the sampling orifice. The instrument has a resolving power of 10,000 (FWHM definition) at *m/z* 500. Voltage settings and acquisition parameters are as previously described[54]. Briefly, the RF ion guide voltage was set at 500 V and the detector voltage set at 2200 V. For negative ion mode, the atmospheric pressure ionization interface potentials were as follows: orifice 1 = -40 V, orifice 2 = -5 V, ring lens = -10 V. For positive ion mode, the following parameters were used: orifice 1 = 40 V, orifice 2 = 5 V, ring lens = 10 V. Mass spectra were stored at a rate of one spectrum per second with an acquired *m/z* range of 100 – 1000. The DART interface was operated in positive ion mode for FAME profiles or negative ion mode for ozonolysis products using helium gas with the gas heater set to 300 °C. For temperature dependency experiments, the stream was set at 150, 200, 250, 300, 350, or 400 °C.

For direct probe analysis, 1 μL of solution was placed on a clean borosilicate glass capillary (World Precision Instruments, Sarasota, FL). For quantitative measurements of isobaric mixtures and fatty acid extracts, samples were introduced into the ion source using DART QuickStrips (IonSense) together with a DART SVP linear rail system. Seven replicates, each 1 μL, were applied to the DART QuickStrip. Immediately after, the strip was placed on the linear movable rail and moved through the ion source at 1 mm/ sec at a distance of 0.5 cm from the inlet.

Calibration for exact mass measurements was accomplished by acquiring a mass spectrum of polyethylene glycol (average molecular weight 600) as an external reference standard in every data file. Analysis was done with JEOL MassCenter software (version 1.3.0.1). Accurate mass measures and isotope pattern matching by MassMountaineer (massmountaineer.com) were used to support elemental composition assignments.

Gas chromatography mass spectrometry (GCMS) analysis was performed on a 7820A GC system equipped with a 5975 Mass Selective Detector (Agilent Technologies, Inc., Santa Clara, CA, USA) and a HP-5ms column ((5%-Phenyl)-methylpolysiloxane, 30 m length, 250 μm ID, 0.25 μm film thickness; Agilent Technologies, Inc.). Electron ionization (EI) energy was set at 70 eV. One microliter of the sample was injected in splitless mode and analyzed with helium flow at 1 mL/ min. The following parameters were used: the column was set at 50 °C for 2 min, increased to 9 °C at a rate of 20 °C/min, then increased to 280 °C at a rate of 5 °C/min for 2 min. The MS was set to detect from *m/z* 40 to 550. Chromatograms and spectra were analyzed using MSD ChemStation (Agilent Technologies, Inc.). FAMEs were identified on the basis of retention time and EI fragmentation pattern compared to a commercially available standard (CRM1891, Sigma-Aldrich).

Ozonolysis

Ozone was produced by a portable ozone generator (ACT-300, GreenAir Ozongenerator) with an ozone output of 0.2% O_3/ m^3/ hour in air. Ozone was blown over the capillary glass tube for 5-10 s or the QuickStrip for 20 s immediately before placement in the DART source. For ozone exposure time experiment, ozone was blown over the samples on the QuickStrip for 1, 20, 40, or 60 s. Note that ozone exposure can lead to respiratory tissue damage, throat irritation, and shortness of breath. Ozone generators should be used within a fume hood and while wearing the appropriate personal protective equipment.

Semi-quantification of isobaric molecules in a mixture

The standards 9(*Z*), 12(*Z*)-Linoleic Acid, and 10(*E*), 12(*Z*)-Conjugated Linoleic Acid, each 3 mM, were mixed in ratios of 1:9, 1:2, 1:1, 2:1, and 9:1 (LA:CLA) in hexane. The mixture was spotted on a QuickStrip and exposed to ozone vapor for 20 s. Seven technical replicates were prepared for each ratio.

Statistical classification

Linear discriminant analysis (LDA) and kernel principal component analysis (KPCA) were performed using Mass Mountaineer software. Centroided mass spectra were exported as text

files using MassCenter. A signal threshold of 10% was used to extract features from centroided mass spectral data. For the O_3-FAME analysis, 12 *m/z* values (for LDA) and 21 *m/z* values (for KPCA) with a mass tolerance of 8 mmu were used in the training set. For the non-O_3 data set, 15 *m/z* values (for LDA) and 13 *m/z* values (for KPCA) with a mass tolerance of 8 mmu were used for the training set. The normalized relative abundance of each of the features was calculated relative to the highest intensity peak for the spectrum. Seven technical replicates were averaged to generate an average profile from each biological replicate. Three to five biological replicates were obtained for each species. Leave one out cross validation (LOOCV) was used to validate the predictive model based on the initial data set. LOOCV is a common form of cross-validation wherein the predictive model is applied to different partitions of the data set. To do so, the model derived from the original training set is applied to training sets from which a single observation is omitted. The process of omission is repeated for the set of all observations. The validation results are averaged resulting in a score (0-100%) that estimates the predictive performance of the model.

Results and Discussion

Ozonolysis coupled with DART MS analysis of oleic acid (OA), linoleic acid (LA), conjugated linoleic acid (CLA), and a *Drosophila* fatty alcohol pheromone CH503 yielded carboxylate and aldehyde products with *m/z* values diagnostic of carbon-carbon double bond positions (Figure 1). Ozonolysis of OA produced major fragments at *m/z* 171.11 and 187.10, each corresponding to the dissociation of the oleic acid backbone at the carbon-9 (C9) position (Figure 1A). Minor signals for the fragment from the terminal methyl end (*m/z* 157.12 and 141.12) were also be observed. Isobaric molecules could also be differentiated on the basis of distinct O_3-DART-induced fragmentation ions, as shown with our analyses comparing LA to CLA (Figure 1B, C). O_3-DART analysis of LA, which contains double bonds at C9 and C12, resulted in carboxylic and ketone products corresponding to the loss of 6 (*n*-6) or 9 (*n*-9) carbons and a signal matching the ozonide (*m/z* 375.21). In addition, dimethoxy products corresponding to the methylene spacing between double bonds at *m/z* 103.00 were present. By contrast, O_3-DART analysis of CLA, which contains double bonds at C10 and C12, resulted in fragments indicative of a 6 or 8

carbon loss from the intact molecule. In the absence of O_3 exposure, signals corresponding to ozonolysis-related fragments were not detected (data not shown), indicating that under our experimental conditions, ambient O_3 has a negligible effect carbon-carbon double bond cleavage.

To determine whether the presence of multiple functional groups and non-conjugated double bonds influence ozonolysis-induced dissociation, we analyzed a natural fatty alcohol product, the *Drosophila* sex pheromone, CH503 [(3*R,*11*Z,*19*Z)-3-acetoxy-11,19-octacosadien-1-ol*] that contains two carbon-carbon double bonds, a terminal alcohol, and an acetyl functional group (Figure 1D). Ozonolysis of CH503 isolated from crude extract was previously performed using conventional work-up conditions, allowing side-by-side comparisons of O_3-DART with a standard ozonolysis protocol[55]. Ozone-induced fragments corresponding to the aldehyde and carboxylic acid anions of each of the three expected fragments were observed. A dimethoxy C8 fragment also was identified (*m/z* 157.09), corresponding to the portion of the intact molecule that is flanked on both termini by double bonds. The product ions are identical to previous ozonolysis reactions with CH503 followed by base hydrolysis and GCMS analysis[55] .

To determine how O_3 exposure time or DART stream temperature affected ozonolysis, we used CLA as a standard and varied exposure time to ozone, ranging from 1 to 60 s, or DART stream temperature, ranging from 250 - 450 °C. Ozone exposure for as brief as 1 s was sufficient to a produce a near-complete breakdown of the intact molecule, as indicated by the near absence of the parent ion at *m/z* 279.23, and the presence of the major aldehyde ion at *m/z* 185.12, and carboxylic product at *m/z* 201.12 (Figure 2A). With increasing ozone exposure time, the overall abundance of the *m/z* 185.12 peak decreased, possibly due to decomposition induced by reactions with water, OH radicals, or other reactive species[56]. The mildest DART stream temperature conditions tested (150 °C) resulted in the highest abundance of the cleavage products (Figure 2B). Increasing DART stream temperature may accelerate rapid thermal decomposition of labile fragments.

Semi-quantitation of regioisomers in a mixture

FAs that have the same number of carbons but different double bond positions cannot be distinguished using MS and are difficult to resolve using low-energy CID. To examine whether

O_3-DART could be used to determine the relative quantities of isobaric FAs in a mixture, we analyzed mixtures of LA and CLA in 5 different ratios following ozone exposure and calculated the relative intensities of diagnostic ions corresponding to cleavage at C9 (*m/z* 171.10) or C10 (*m/z* 185.12) (Figure 3). The relative intensities of ions corresponding to *n*-9 and *n*-8 aldehydes reflected the molar ratio of the 2 isobaric species in a linear manner ($R^2 = 0.99$). The results reveal that diagnostic fragments of isobaric species resulting from O_3-DART can be used to quantify relative levels of each species in a mixture without prior separation.

Analysis of complex fatty acid mixtures with O_3*-DART improves species classification*

Amongst natural populations, there can also be substantial variation in the double bond positions of FAs due to the influence of diet, health, and genetic background[12, 13, 16-18]. Having established that O_3-induced fragmentation accurately reflects the relative ratios of isobaric molecules in a mixture, we examined whether this feature could aid in the classification of closely related animal populations or species. We used DART MS with and without ozonolysis to determine whether fatty acid profiles can distinguish between drosophilid species and between different populations of the same species. The chemical profiles generated from both FA methyl ester (FAME) and ozone-treated FAME extracts were used as features in linear discriminant analysis. Each species could be distinguished on the basis of FAME and FAME positional isomer profiles using linear discriminant analysis (LDA; Figure 4, Supplemental Table 1). To confirm the double bond position of the precursor FAs, the same methylated extracts were analyzed by GCMS. GCMS analyses revealed thirteen major FAMEs and the double bond positions were confirmed by comparison to commercially available FAME standards (Supplemental Table 2). Leave one out cross validation (LOOCV) applied to the FAME or O_3-FAME profiles showed that each model accurately predicted species with 82% and 91% accuracy, respectively. LDA using O_3-FAME features resulted in a clearer separation between each species, indicating that drosophilids can exhibit a species-specific FA positional isomer signature. Notably, the O_3-FA profile can be used to distinguish between two populations of the same species (*D. silvestris*) that were collected in separate sites. Cluster analysis using a non-supervised method, kernel principal analysis (KPCA), gave similar results: FAME profiles did not show robust species-specific groups (LOOCV: 43%) whereas O_3-FAME data improved categorization (LOOCV: 76%;

Supplemental Figure 1). In the absence of chromatographic separation and ion isolation, it was not possible to assign ozonolysis products to the respective precursors. Thus, whether isomeric variation is due to FAs of a particular carbon length or is common to multiple unsaturated FAs cannot be distinguished. Nonetheless, our results reveal that distinct FA unsaturation profiles can be used to separate closely related taxa and the differences may reflect distinct dietary habits, metabolic pathways, or an evolutionary response to environmental conditions such as humidity and temperature[57].

Conclusions

The combination of ozonolysis with DART MS analysis provides a method for the straightforward determination of double bond position in lipids without the need for a subsequent oxidative-workup or tandem mass spectrometry. A notable limitation of the method as presented is that in the absence of chromatographic separation or ion isolation it is not possible to assign double bond position to individual lipid species in a complex mixture. Nevertheless, the unsaturation profile produced from complex samples such as fatty acid extracts can be helpful for rapid animal species differentiation. Furthermore, this method will be useful for structural elucidation of purified natural products such as pheromones and other lipid signaling molecules.

Conflicts of interest

RBC is an employee of JEOL USA, the manufacturer of the AccuTOF MS instrument and the author of Mass Mountaineer software.

Acknowledgements

This work was supported by the Department of Defense, U.S. Army Research Office (W911NF1610216 to J.Y.Y), National Institutes of Health (1P20GM125508 to J.Y.Y.), and the Singapore National Research Foundation (NRF-RF2010-06 to JY.Y.). We thank Kenneth

Kaneshiro, Kelvin Kanegawa, and the Hawaiian Drosophila Research Stock Center for providing fly samples.

References

1. F. M. Goni, L. R. Montes and A. Alonso, *Prog Lipid Res*, 2012, **51**, 238-266.
2. A. G. Lee, *Trends Biochem Sci*, 2011, **36**, 493-500.
3. P. J. Quinn, *Prog Lipid Res*, 2012, **51**, 179-198.
4. J. Y. Yew and H. Chung, *Prog Lipid Res*, 2015, **59**, 88-105.
5. S. Ishikawa, I. Tateya, T. Hayasaka, N. Masaki, Y. Takizawa, S. Ohno, T. Kojima, Y. Kitani, M. Kitamura, S. Hirano, M. Setou and J. Ito, *PLoS One*, 2012, **7**, e48873.
6. D. Touboul and M. Gaudin, *Bioanalysis*, 2014, **6**, 541-561.
7. Y. Liu, Y. Chen, A. Momin, R. Shaner, E. Wang, N. J. Bowen, L. V. Matyunina, L. D. Walker, J. F. McDonald, M. C. Sullards and A. H. Merrill, Jr., *Mol Cancer*, 2010, **9**, 186.
8. S. M. Willems, A. van Remoortere, R. van Zeijl, A. M. Deelder, L. A. McDonnell and P. C. Hogendoorn, *J Pathol*, 2010, **222**, 400-409.
9. H. Ruh, T. Salonikios, J. Fuchser, M. Schwartz, C. Sticht, C. Hochheim, B. Wirnitzer, N. Gretz and C. Hopf, *J Lipid Res*, 2013, **54**, 2785-2794.
10. M. Munoz-Culla, H. Irizar and D. Otaegui, *Appl Clin Genet*, 2013, **6**, 63-73.
11. M. T. Nakamura and T. Y. Nara, *Annu Rev Nutr*, 2004, **24**, 345-376.
12. H. L. Wang, M. A. Lienard, C. H. Zhao, C. Z. Wang and C. Lofstedt, *Insect Biochem. Mol. Biol.*, 2010, **40**, 742-751.
13. M. Serra, B. Pina, J. L. Abad, F. Camps and G. Fabrias, *Proc Natl Acad Sci U S A*, 2007, **104**, 16444-16449.
14. H. Jabeur, A. Zribi, J. Makni, A. Rebai, R. Abdelhedi and M. Bouaziz, *J Agric Food Chem*, 2014, **62**, 4893-4904.
15. U. Riserus, W. C. Willett and F. B. Hu, *Prog Lipid Res*, 2009, **48**, 44-51.
16. A. Erkkila, V. D. de Mello, U. Riserus and D. E. Laaksonen, *Prog Lipid Res*, 2008, **47**, 172-187.
17. L. Hodson, C. M. Skeaff and B. A. Fielding, *Prog Lipid Res*, 2008, **47**, 348-380.
18. A. Baylin, E. K. Kabagambe, X. Siles and H. Campos, *Am J Clin Nutr*, 2002, **76**, 750-757.
19. C. Cheng, M. L. Gross and E. Pittenauer, *Anal Chem*, 1998, **70**, 4417-4426.
20. E. Pittenauer and G. Allmaier, *J Am Soc Mass Spectrom*, 2009, **20**, 1037-1047.

21. F. F. Hsu and J. Turk, *J Am Soc Mass Spectrom*, 2008, **19**, 1681-1691.
22. F. F. Hsu and J. Turk, *J Am Soc Mass Spectrom*, 2008, **19**, 1673-1680.
23. A. Kubo, T. Satoh, Y. Itoh, M. Hashimoto, J. Tamura and R. B. Cody, *J Am Soc Mass Spectrom*, 2013, **24**, 684-689.
24. H. Takahashi, Y. Shimabukuro, D. Asakawa, S. Yamauchi, S. Sekiya, S. Iwamoto, M. Wada and K. Tanaka, *Anal Chem*, 2018, **90**, 7230-7238.
25. Y. Zhao, H. Zhao, X. Zhao, J. Jia, Q. Ma, S. Zhang, X. Zhang, H. Chiba, S. P. Hui and X. Ma, *Anal Chem*, 2017, **89**, 10270-10278.
26. X. Zhao, Y. Zhao, L. Zhang, X. Ma, S. Zhang and X. Zhang, *Anal Chem*, 2018, **90**, 2070-2078.
27. Y. Xu and J. T. Brenna, *Anal Chem*, 2007, **79**, 2525-2536.
28. X. Ma and Y. Xia, *Angew Chem Int Ed Engl*, 2014, **53**, 2592-2596.
29. X. Ma, L. Chong, R. Tian, R. Shi, T. Y. Hu, Z. Ouyang and Y. Xia, *Proc Natl Acad Sci U S A*, 2016, **113**, 2573-2578.
30. T. Xu, Z. Pi, F. Song, S. Liu and Z. Liu, *Anal Chim Acta*, 2018, **1028**, 32-44.
31. W. Zhang, D. Zhang, Q. Chen, J. Wu, Z. Ouyang and Y. Xia, *Nat Commun*, 2019, **10**, 79.
32. A. Bednarik, S. Bolsker, J. Soltwisch and K. Dreisewerd, *Angew Chem Int Ed Engl*, 2018, **57**, 12092-12096.
33. R. Criegee, *Angew Chem*, 1975, **14**, 745-752.
34. K. A. Harrison and R. C. Murphy, *Anal Chem*, 1996, **68**, 3224-3230.
35. S. R. Ellis, J. R. Hughes, T. W. Mitchell, M. in het Panhuis and S. J. Blanksby, *Analyst*, 2011, **137**, 1100-1110.
36. J. I. Zhang, W. A. Tao and R. G. Cooks, *Anal Chem*, 2011, **83**, 4738-4744.
37. M. C. Thomas, T. W. Mitchell, D. G. Harman, J. M. Deeley, J. R. Nealon and S. J. Blanksby, *Anal Chem*, 2008, **80**, 303-311.
38. M. C. Thomas, T. W. Mitchell, D. G. Harman, J. M. Deeley, R. C. Murphy and S. J. Blanksby, *Anal Chem*, 2007, **79**, 5013-5022.
39. M. R. L. Paine, B. L. J. Poad, G. B. Eijkel, D. L. Marshall, S. J. Blanksby, R. M. A. Heeren and S. R. Ellis, *Angew Chem Int Ed Engl*, 2018, **57**, 10530-10534.

40. D. L. Marshall, A. Criscuolo, R. S. E. Young, B. L. J. Poad, M. Zeller, G. E. Reid, T. W. Mitchell and S. J. Blanksby, *J Am Soc Mass Spectrom*, 2019, DOI: 10.1007/s13361-019-02261-z.
41. B. L. J. Poad, X. Zheng, T. W. Mitchell, R. D. Smith, E. S. Baker and S. J. Blanksby, *Anal Chem*, 2018, **90**, 1292-1300.
42. R. L. Kozlowski, J. L. Campbell, T. W. Mitchell and S. J. Blanksby, *Anal Bioanal Chem*, 2015, **407**, 5053-5064.
43. B. L. Poad, H. T. Pham, M. C. Thomas, J. R. Nealon, J. L. Campbell, T. W. Mitchell and S. J. Blanksby, *J Am Soc Mass Spectrom*, 2010, **21**, 1989-1999.
44. H. I. Kim, H. Kim, Y. S. Shin, L. W. Beegle, W. A. Goddard, J. R. Heath, I. Kanik and J. L. Beauchamp, *J Phys Chem B*, 2010, **114**, 9496-9503.
45. J. Y. Ko, S. M. Choi, Y. M. Rhee, J. L. Beauchamp and H. I. Kim, *J Am Soc Mass Spectrom*, 2012, **23**, 141-152.
46. C. A. Stinson, W. Zhang and Y. Xia, *J. Am. Soc. Mass Spectrom.*, 2018, **29**, 481-489.
47. C. Sun, Y. Y. Zhao and J. M. Curtis, *Anal Chim Acta*, 2013, **762**, 68-75.
48. C. Sun, Y. Y. Zhao and J. M. Curtis, *J Chromatogr A*, 2014, **1351**, 37-45.
49. C. Sun, Y. Y. Zhao and J. M. Curtis, *J Agric Food Chem*, 2015, **63**, 1442-1451.
50. R. A. Harris, J. C. May, C. A. Stinson, Y. Xia and J. A. McLean, *Anal Chem*, 2018, **90**, 1915-1924.
51. S. D. Maleknia and K. M. Downard, *Chem Soc Rev*, 2014, **43**, 3244-3258.
52. K. Mori, Y. Shikichi, S. Shankar and J. Y. Yew, *Tetrahedron*, 2010, **66**, 7161-7168.
53. M. R. Wheeler and F. E. Clayton, *Dros Inf Serv*, 1965, **40**, 98.
54. R. B. Cody and A. J. Dane, *J Am Soc Mass Spectrom*, 2013, **24**, 329-334.
55. J. Y. Yew, K. Dreisewerd, H. Luftmann, J. Muthing, G. Pohlentz and E. A. Kravitz, *Curr Biol*, 2009, **19**, 1245-1254.
56. R. Wegener, T. Brauers, R. Koppmann, S. Rodríguez Bares, F. Rohrer, R. Tillmann, A. Wahner, A. Hansel and A. Wisthaler, *J Geophys Res Atmos*, 2007, **112**.
57. K. L. Uy, R. LeDuc, C. Ganote and D. K. Price, *Conserv Physiol*, 2015, **3**, cou062.

Figure legends

Figure 1

Negative ion DART MS mass spectra of fatty acids and fatty alcohol standards following brief exposure to ozone vapor. (A) Oleic acid [(9Z)-Octadecenoic acid]; (B) linoleic acid [(9Z,12Z)-octadecadienoic acid]; (C) conjugated linoleic acid [(10Z,12Z)-octadecadienoic acid]; (D) CH503 [(3*R*,11*Z*,19*Z*)-3-acetoxy-11,19-octacosadien-1-ol]. Diagnostic carboxylate and aldehyde ozonolysis product ions indicative of double bond position (labeled with '*') match the predicted fragmentation products. The "*n*" label used to denote ozone-induced fragmentation indicates the loss of carbons from the terminal methyl carbon.

Figure 2

Conjugated linoleic acid ozonolysis product formation as a function of O_3 exposure time and DART stream temperature. Each point represents the average normalized abundance of 7 replicates and error bars indicate standard error. (A) Cleavage products are observed within 1 s of O_3 exposure. Abundance of diagnostic fragments drops significantly after 20 s of O_3 exposure; ANOVA with Holm-Sidak multiple comparison test comparing fragment abundance at 20, 40, or 60 s to 1 s; ns: not significant. (B) DART stream temperatures above 150 °C accelerate the breakdown of ozonide products; ANOVA with Holm-Sidak multiple comparison test, comparing fragment abundance at 200 °C and above to 150 °C.

Figure 3

Relative quantification of double bond positional isomers in a mixture based on the abundance of diagnostic ozone-derived ions. (A) Representative DART MS spectra of a 1:1 mixture of LA and CLA following O_3 exposure shows distinct fragments for each of the double bond regioisomers.

(B) Relative abundances of diagnostic ions reflect the LA: CLA molar ratio. Regression analysis with a linear model reveals an R^2 value of 0.99.

Figure 4

Fatty acid unsaturation profiles distinguish different species and different populations of the same species. (A) Mirrored DART MS spectra of *Drosophila heteroneura* (top) and *D. silvestris* FAME extracts (bottom) in positive ion mode reveals a series of medium chain fatty acid methyl esters with 0-3 double bonds (notation indicates number of carbons: number of double bonds). FA identities were confirmed by parallel analysis with GCMS. (B) Mirrored O_3-DART MS spectra of FAME extracts in negative ion mode contain a mixture of carboxylic and aldehyde product ions. Signals corresponding to major cleavage products are labeled with putative double bond positions, inferred by GCMS analysis (Supplemental Tables 1, 2). Species-specific differences are apparent in the profiles (outlined). (C, D) Linear discriminant analysis using FAME or O_3-FAME profiles shows improved classification of each *Drosophila* species with the use of ozonolysis-derived signals. The LOOCV testing was 82% and 91%, respectively, for LDA classification model analysis with FAME or O_3-FAME features; Dsil_p1: *D. silvestris*, population 1; Dsil_p2: *D. silvestris*, population 2; Ddif: *D. differens*; Dhem: *D. hemipeza*; Dhet: *D. heteroneura*; Dgri: *D. grimshawi*.

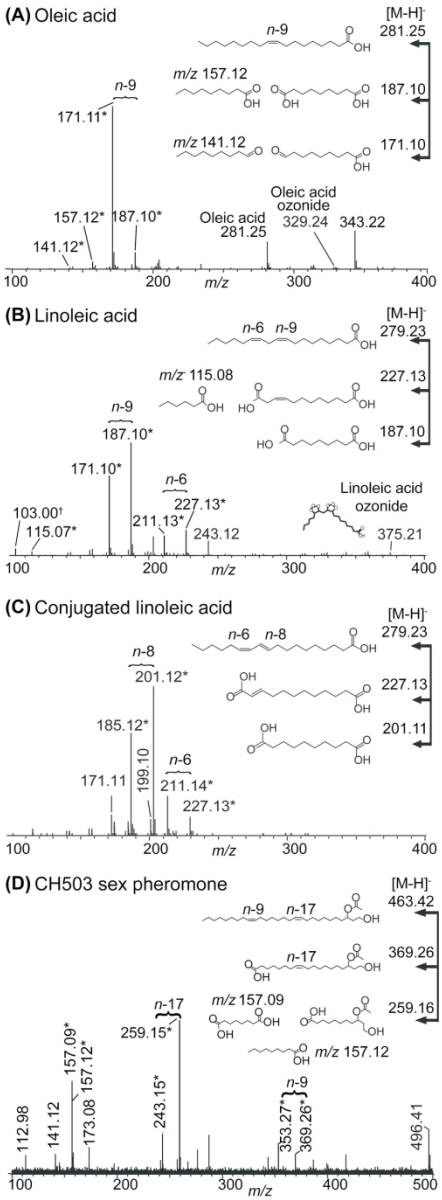

81x225mm (300 x 300 DPI)

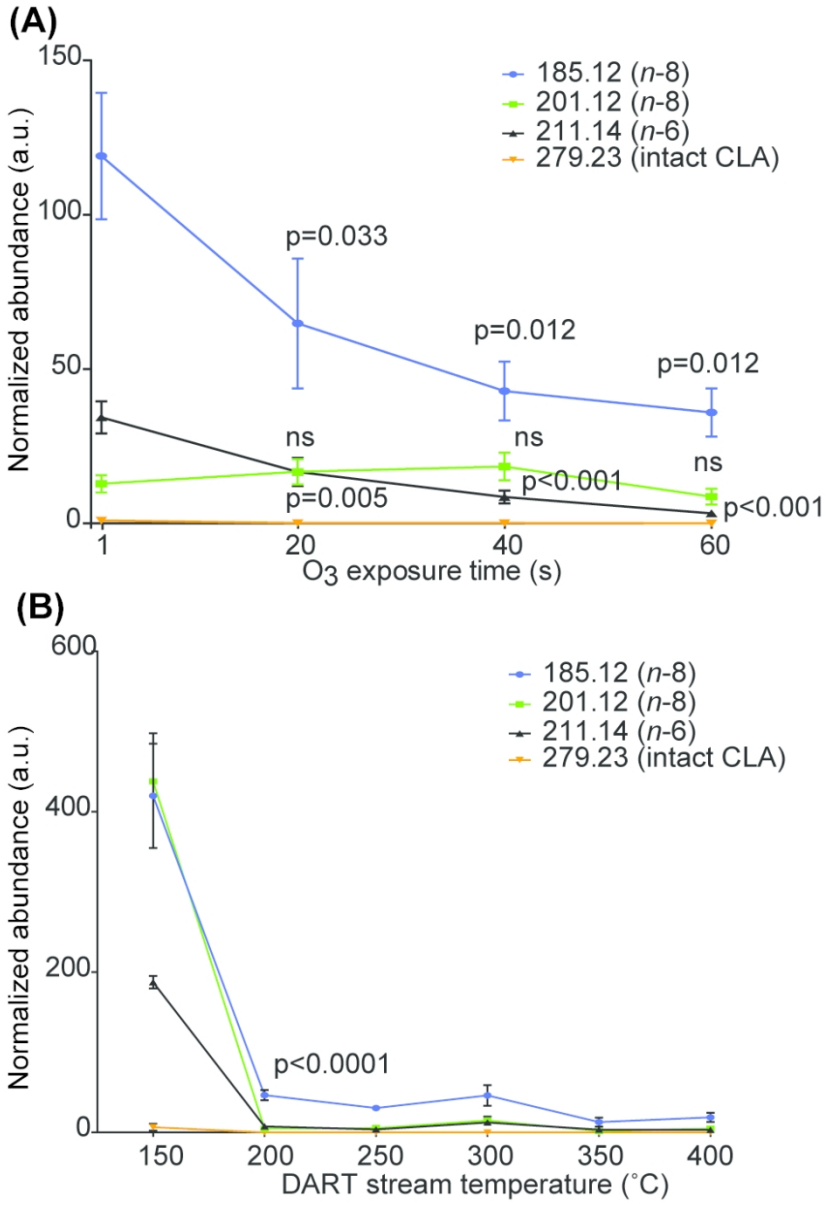

82x119mm (300 x 300 DPI)

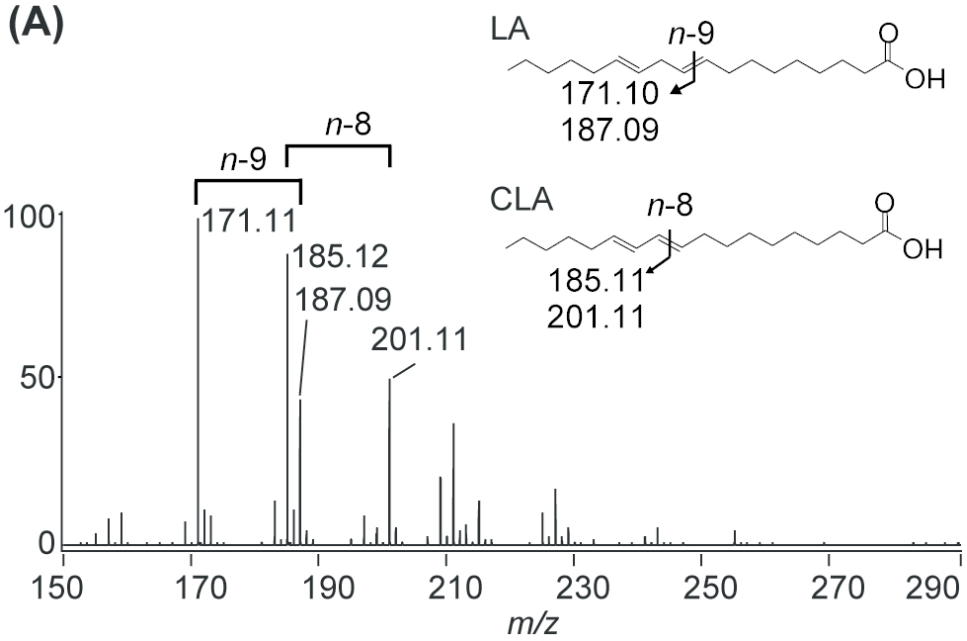

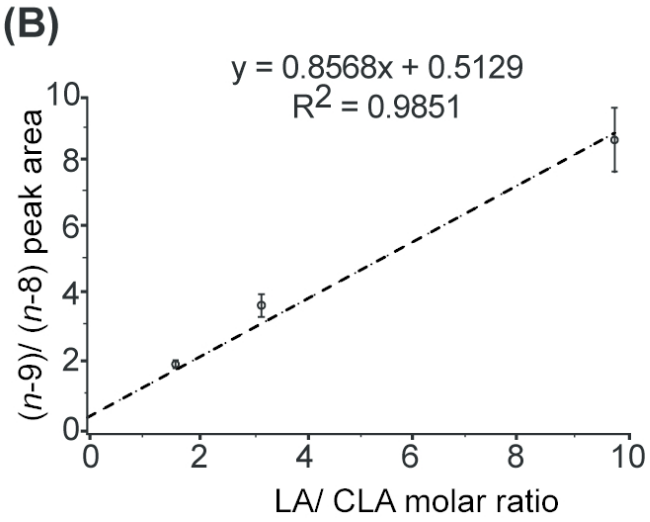

82x102mm (300 x 300 DPI)

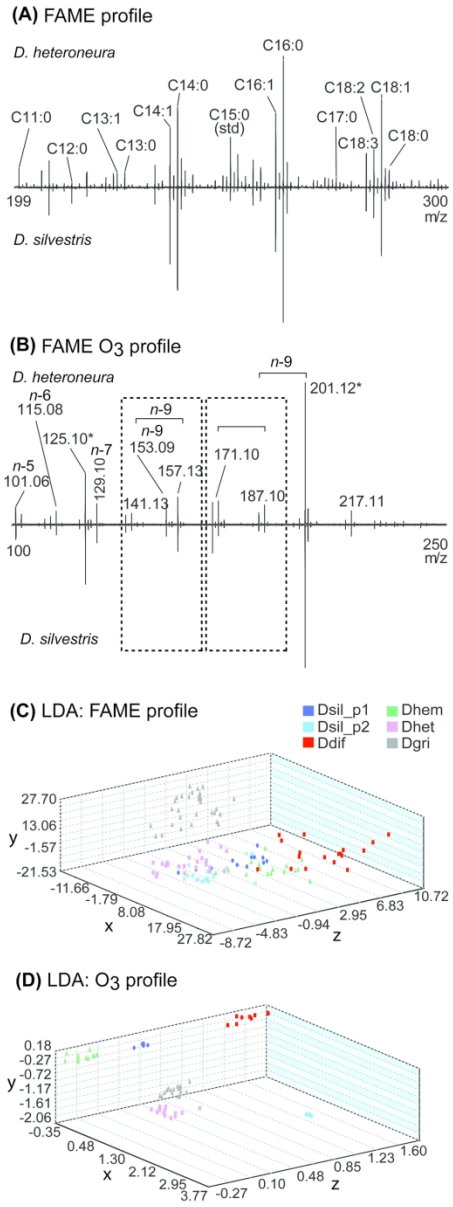

82x221mm (300 x 300 DPI)